Available online at www.sciencedirect.com

ScienceDirect

Focus Article, *Mendeleev Commun.*, 2019, **29**, 121–127

Mendeleev Communications

Non-covalent interactions in stoichiometric and catalytic reactions of iridium pincer complexes

Elena S. Osipova, Oleg A. Filippov, Elena S. Shubina and Natalia V. Belkova*

A. N. Nesmeyanov Institute of Organoelement Compounds, Russian Academy of Sciences, 119991 Moscow, Russian Federation. E-mail: nataliabelk@ineos.ac.ru

DOI: 10.1016/j.mencom.2019.03.001

Recent results in the chemistry of various pincer Ir^{III} complexes are highlighted with the particular attention paid to the activation of Ir–Cl and Z–H bonds (Z–H = M–H, B–H, N–H, *etc*.) *via* low-energy (non-covalent) interactions (hydrogen bonded or Lewis complexes) and the role of such interactions in the proposed mechanisms of amine–borane dehydrogenation reaction.

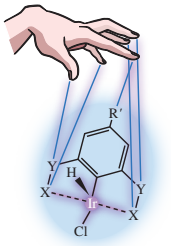

Introduction

Nowadays, hydrogen bonds and other non-covalent interactions are well recognized as very important for both chemistry and biochemistry, in catalytic and stoichiometric reactions, as well as in the design of supramolecular systems and materials. Investigating hydrogen bonds involving those in complexes of transition metals and hydrides of main group elements, we have established the spectral criteria, structural and electronic parameters of dihydrogen bonds formation ($M–H^{\delta-}\cdots^{\delta+}H–A$), determined their properties, and revealed their key role in the reaction of metal hydrides with organic acids (H–A).[1–3] It is well known that being the first step of proton transfer from an acid A–H to a base Y, the formation of the hydrogen bond $AH^{\delta+}\cdots Y$ results in the activation of the A–H bond. In the case of metal hydrides as bases, the dihydrogen bond formation activates both interacting Z–H bonds (*i.e*., M–H and A–H).[4] Therefore, the reaction between metal hydrides (M–H) and acids (A–H) proceeds as a concerted proton and hydride transfer. The hydrogen and dihydrogen bonds formation and the subsequent proton and hydride transfer are essential not only for stoichiometric reactions of metal hydrides

Elena S. Osipova received her MS at Chemistry Department of M. V. Lomonosov Moscow State University in 2014 and continued her education by admission to the PhD program at the A. N. Nesmeyanov Institute of Organoelement Compounds of the Russian Academy of Sciences (in the Laboratory of Metal Hydrides) under supervision of Professors Elena Shubina and Natalia Belkova. In 2016, she completed a training in the group of Dr. Maurizio Peruzzini at the Institute of Chemistry of OrganoMetallic Compounds ICCOM-CNR (Florence, Italy).

Oleg A. Filippov received his MS (1999) and PhD (2003) degrees at M. V. Lomonosov Moscow State University. Since 2002, he is a member of Laboratory of Metal Hydrides at the A. N. Nesmeyanov Institute of Organoelement Compounds of the Russian Academy of Sciences. In 2007–2008, he attended a post-doctoral training in the group of Professor Agustí Lledós at Universitat Autònoma de Barcelona (Spain). In 2017, he received Dr.Sci. degree being currently a senior researcher in the Laboratory of Metal Hydrides at A. N. Nesmeyanov Institute of Organoelement Compounds of the Russian Academy of Sciences, specializing in computational chemistry and molecular spectroscopy, and their applications to the main group element compounds and hydrides, intermolecular interactions, hydrogen bonding, and proton transfer as well as other reaction mechanisms.

Elena S. Shubina graduated from M. V. Lomonosov Moscow State University and received her PhD degree there. She completed her Dr.Sci degree at the A. N. Nesmeyanov Institute of Organoelement Compounds of the Russian Academy of Sciences, where she is a Professor of Chemistry and the head of the Metal Hydrides Laboratory since 2001. She was plenary, invited or keynote lecturer at European and International Conferences on organometallic, coordination and boron chemistry. She is a member of EuCheMS Division on Organometallic Chemistry. Fields of her research interest include physical organoelement chemistry, molecular spectroscopy, non-covalent interactions involving metal complexes, transition metal and main group element hydrides, and supramolecular compositions. She has published over 150 papers in Russian and international journals and several book chapters.

Natalia V. Belkova graduated from M. V. Lomonosov Moscow State University and received the PhD degree at A. N. Nesmeyanov Institute of Organoelement Compounds of the Russian Academy of Sciences. Her PhD work had been awarded by Academia Europeae award for young scientists from Russia in 1997. After two years post-doctoral fellowship at St. Jude Children's Research Hospital (Memphis, TN, USA), she returned to the A. N. Nesmeyanov Institute, where she received her Dr.Sci. degree in 2011 and became a leading researcher. In 2016, she was elected a Professor of Russian Academy of Sciences. Her research interests include hydrogen bonding and other non-covalent interactions in organometallic chemistry and their implication in mechanisms of reactions involving migration of hydrogen ions (proton transfer, hydride transfer), and structure–properties relationships for metal complexes.

with acids, but also are the key steps in catalytic hydrogenation reactions of multiple bonds by transition metal complexes.[1,5,6]

To date, hydride complexes of transition metals and boron compounds, *e.g.*, amine–boranes RR′NH·BH_3, attract the attention of researchers as catalysts for dehydrogenation and starting compounds for the hydrogen storage systems,[7,8] and also as promising objects for the design of BN ceramics and new polymeric materials.[9,10] At this end, the catalytic dehydrogenation of amine–boranes is still of great interest despite the difficulties of re-hydrogenating the amine–borane,[11,12] and a huge number of systems are reported.[13–17] Interestingly, the iridium pincer complex ($^{Bu^t}$POCOP)IrH_2 well-known as the catalyst for the dehydrogenation of alkanes[18] remains one of the most efficient catalysts for the dehydrogenation of amine–boranes.[19]

The chemistry of pincer ligated metal complexes has experienced tremendous development and been applied to various stoichiometric and catalytic chemical transformations. The term 'pincer ligand' was originally referred to species of the type [2,6-$(ECH_2)C_6H_3$]$^-$ bearing the anionic central carbon and neutral two-electron donors (E), particularly PR_2 (as shown in the structure **1**) or NR_2.[20] Such ligand structure rigidly determines the meridional geometry relative to the metal center. However, the term 'pincer' is currently applied to any ligand that chelates the metal center in the meridional tridentate configuration.[21] Such coordination of pincer ligands ensures strong binding to the metal center and high stability of the resulting metal complex. Consequently, the high thermal stability of such complexes is one of the key properties determining their efficiency as catalysts for strongly endothermic reactions. In particular, the iridium complexes with PCP and POCOP ligands are the unsurpassed catalysts for the dehydrogenation of alkanes.[21–23]

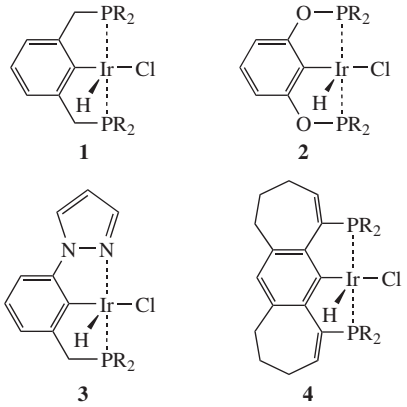

Pincer ligated Ir^{III} complexes are typically obtained by cyclometallation, but the resulting hydrido chloride complexes are usually utilized only as precursors for the corresponding hydrides (Scheme 1). Our recent studies of the 'classic' pincer complex (^{tBu}PCP)IrH(Cl) [**1**; ^{tBu}PCP = κ^3-2,6-$(CH_2PBu^t_2)_2C_6H_3$] revealed that the hydrido chloride complex can also be a useful model to investigate interactions with coordinating solvents and proton donors HA.[24,25] Moreover, complex **1** was quite active in the dehydrogenation of $NHMe_2BH_3$ (DMAB), which allowed us to conduct a spectral study (NMR and IR) of the reaction mechanism.[26]

This review is devoted to (i) the analysis of the recently obtained spectral and theoretical data on various pincer Ir^{III} complexes and the features of their electronic structure, (ii) some aspects of the activation of Z–H and Ir–Cl bonds due to the low-energy (non-covalent) interactions (*e.g.*, hydrogen bonded or Lewis complexes), and (iii) the role of such interactions in proposed mechanisms for the amine–borane dehydrogenation reaction.

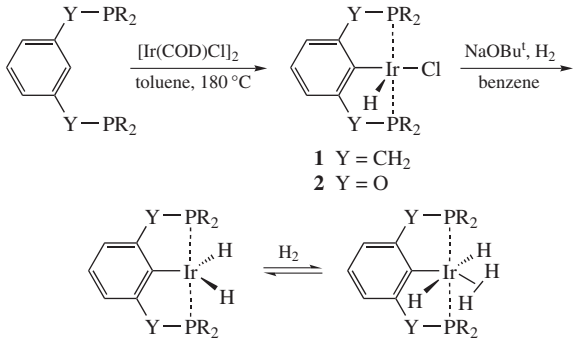

Scheme 1

Structural features of pentacoordinated complexes

According to the X-ray diffraction studies, five-coordinated iridium hydridochloride complexes possess a square-pyramidal geometry, wherein the hydride occupies an apical position, and the donor atoms of the pincer ligand and chloride form the base plane of the pyramid (Figure 1). Analysis of the CCSD database gave only a few analogs of complexes **1** and **2** (Tables 1 and 2). Perusal of these data reveals that the replacement of bridged CH_2 groups in $^{Bu^t}$PCP by oxygen atoms [complex **2**, $^{Bu^t}$POCOP = = κ^3-2,6-$(O\text{-}PBu^t_2)_2C_6H_3$] and the introduction of substituents into the benzene ring lead to rather minor changes of the major structural parameters, slightly affecting mostly the Ir–Cl bond (see Tables 1 and 2). Interestingly, the introduction of a tricyclic pincer ligand (7-6-7-$^{Pr^i}$PCP) (complex **4**, see Table 1 and Figure 1) results in a deviation of the chloride ligand from the PCP plane [the angle C–Ir–Cl becomes 153.5° (**4**) instead of 179° (**1** and **2**), see

Table 1 Selected bond distances (Å) and angles (°) for ($^{Bu^t}$PCP)IrH(Cl) **1** and its congeners according to single crystal X-ray diffraction data.

Parameter	Compound				
	1	**1**-NO_2[a]	**3**	**4** (Pr^i)[b]	**4** (Pr^i) C_6H_6[c]
CCDC no.	757294	145421	1838328	897993	897994
Reference	27	28	29	30	30
Ir–H	1.604		1.5	1.485	1.41
Ir–Cl	2.425	2.440	2.448	2.400	2.378
Ir–C	2.014	2.015	1.99	2.027	2.023
Ir–P(1)	2.305	2.311	2.256	2.273	2.282
Ir–P(2)	2.305	2.314		2.274	2.289
Ir–N			2.07		
H–Ir–Cl	89.44		97.7	127.81	130.38
Cl–Ir–C	179.77	179.32	170.86	153.47	155.47

[a] *p*-NO_2 derivative of **1**. [b] R = Pr^i. [c] Benzene solvate of **4** (Pr^i).

Table 2 Selected bond distances (Å) and angles (°) for ($^{Bu^t}$POCOP)IrH(Cl) **2** and its derivatives according to single crystal X-ray diffraction data.

Parameter	Substituent in benzene ring of complex **2**			
	4-H	3-COOMe, 5-$CH(OMe)_2$	4-NMe_2	4-COOMe
CCDC no.	728028	1431008	1420009	1420010
Reference	31	32	33	33
Ir–H	1.486	1.534	1.299	1.343
Ir–Cl	2.404	2.381	2.396	2.387
Ir–C	2.01	2.008	1.997	1.988
Ir–P(1)	2.293	2.28	2.289	2.294
Ir–P(2)	2.297	2.282	2.294	2.299
H–Ir–Cl	99.94	96.71	95.88	97.88
Cl–Ir–C	179.12	176.39	176.32	172.92
CH···HC	2.676	2.363	2.416	2.446

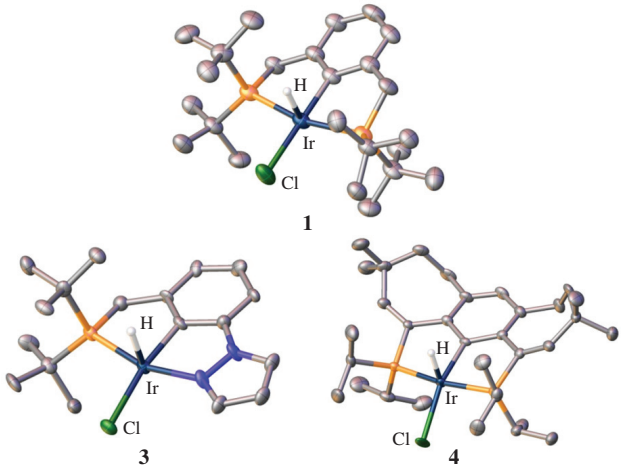

Figure 1 Molecular structures of complexes **1**,[27] **3**,[29] and **4**[30] (the thermal ellipsoids are shown at 50% probability level). Hydrogen atoms of the ligands are omitted for clarity. Color codes: Ir is blue, H is white, Cl is green, P is yellow, and N is magenta.

Tables 1 and 2] and a slight shortening of the Ir–Cl and Ir–P bonds as compared to complex **1**. On the contrary, the replacement of one $CH_2PBu^t_2$ group by a pyrazolate moiety (complex **3**, $^{Bu^t}$PCN = 1-{3-[(di-*tert*-butylphosphino)methyl]phenyl}-1*H*-pyrazole, see Scheme 1) causes a slight elongation of the Ir–Cl and Ir–P bonds and opens access to the hydride and iridium atom (Figure 2). The CH protons of phosphorus decorating groups are in the close proximity to the chloride ligands, but Cl remains exposed (see Figure 2). On the other hand, the empty coordination place in almost all complexes (except for **3**) is shielded by the bulky Bu^t/Pr^i groups, while the shortest CH···HC distance diminishes from 3.397 Å in **1** to 2.676 Å in **2** (see Figure 2) and even below that in the arene-substituted derivatives of **2** (see Table 2). Thus, this direction appears as well protected in the case of $^{Bu^t}$POCOP-pincer ligands.

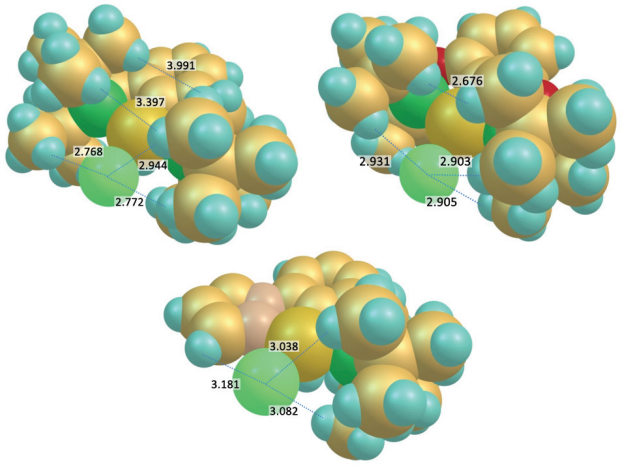

Figure 2 Space-filling structures of hydridochloride complexes **1**–**3**, showing the shortest CH···Cl and CH···HC distances (Å).

Electronic properties of pentacoordinated complexes

The DFT analysis of molecular electrostatic potential (MEP) has been performed for complexes **1**–**3** and a set of the *para*-substituted PCP-based complexes (derivatives of **1** bearing F, CF_3, NO_2, COOMe and OMe groups at the *para*-position of cyclometallated benzene ring).[34] The global MEP minima $V_{S,min}$ were found for the Cl ligand as two extrema points, which correspond to the two occupied *p*-orbitals (Figure 3). This coincides with the location of HOMOs for all the complexes on the chloride

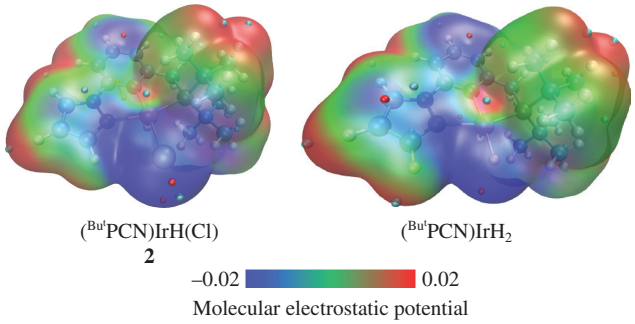

Figure 3 The molecular electrostatic potential distribution for ($^{Bu^t}$PCN)IrH(Cl) **2** and the corresponding dihydride ($^{Bu^t}$PCN)IrH_2 mapped on the VdW surface (isosurface of electron density with isovalue 0.001 a.u.) on the BGR scale (–0.02 – 0.0 – +0.02). The MEP extrema are depicted as red (minima, $V_{S,min}$) and cyan (maxima, $V_{S,max}$) balls.

ligand, the HOMO energy being varied in the relatively narrow range from –6.06 to –5.13 eV. Accordingly, the chloride ligand was experimentally determined as the proton accepting site for hydrogen bonds with OH and NH_2 donors.[24,25] The location of another MEP minimum on the arene ring is in a good agreement with the formation of π···HO hydrogen bond (Figure 4), which was also detected both experimentally and computationally.[25]

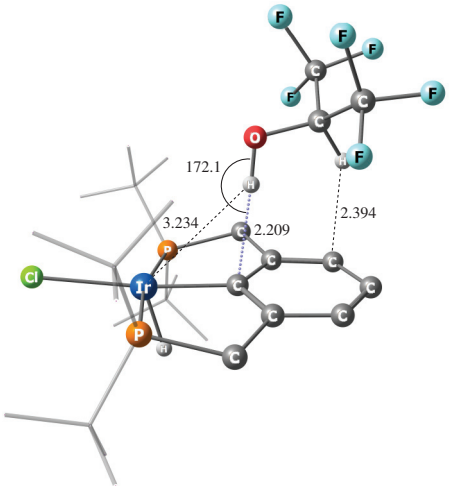

Figure 4 DFT/M06 optimized geometry of one among the hydrogen-bonded adducts between **1** and CF_3CH_2OH, showng the interaction of alcohol with the benzene ring. Hydrogen atoms of the $^{Bu^t}$PCP ligand are omitted for clarity, and the Bu^t groups are shown as a wireframe. Color coding: Ir is azure, P is orange, Cl is green, F is cyan, O is red, C is gray, and H is light gray. Figure from ref. 25. ©2016 Elsevier B.V. Reproduced with permission.

The two local MEP maxima found near the Ir–H line perpendicular to the pincer (PCP) plane could be regarded as parameters characterizing the Lewis acidity of the iridium atom, the higher $V_{S,max}$ value meaning the higher Lewis acidity of metal. The maxima points are located close to the hydride ligand and at the empty coordination place (see Figure 3), the latter coinciding with the LUMO location (Figure 5). Only in the case of *p*-NO_2 substituted complex, the Ir-based orbital is LUMO+1, while the LUMO is located on the NO_2 group.[34] Analysis of the MEP maxima energies $V_{S,max}$ reveals that the substitution at the aromatic ring or replacement of CH_2 bridges by oxygen ones affect the acidity of metal center. For PCP-series, there is a correlation of $V_{S,max}$ with Hammett σ_p constants[35] of the *para*-substituents (Figure 6) wherein the strongest electron-donor, the methoxy group [σ_p(MeO) = –0.27], and the strongest electron-acceptor, the nitro group [$\sigma_p(NO_2)$ = 0.78], flank the metal acidity ($V_{S,max}$)

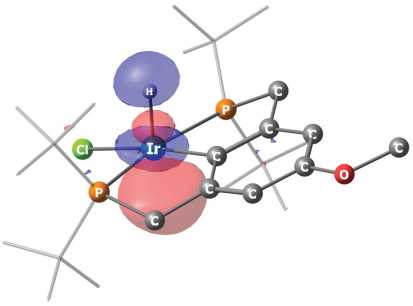

Figure 5 LUMO of *p*-OMe substituted analogue of complex **1** shown as the isosurface at 0.06 a.u. Hydrogen atoms of the $^{Bu^t}$PCP ligand are omitted, and the Bu^t groups are shown as a wireframe.

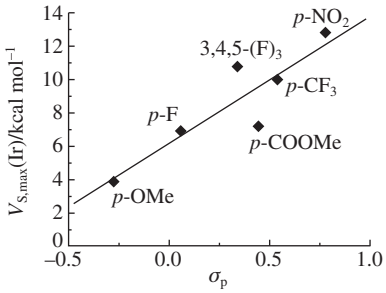

Figure 6 Correlation between MEP maximum energy on iridium and Hammett σ_p parameters of *para*-substituent in the PCP-based complexes; σ_m value is used for trisubstituted complex containing fluorine at 3,4,5-positions of the benzene ring. Data from ref. 34.

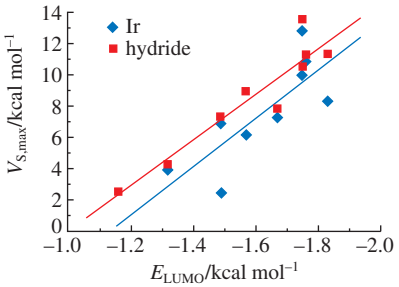

Figure 7 Correlation of MEP maximum energy on iridium and hydride with the LUMO energy for complexes **1**–**3** and *para*-substituted PCP-series. Data from ref. 34.

order. Accumulated data on complexes **1**–**3** and *para*-substituted PCP-series also show the correlation between the LUMO and $V_{S,max}$ energies (Figure 7).

Interestingly, the dihydrides ($^{Bu^t}$PCP)IrH$_2$ and ($^{Bu^t}$PCN)IrH$_2$ (the derivatives of hydridochlorides **1** and **3**, respectively) exhibit the conserved MEP distribution. In the case of L-shaped complexes possessing the original square pyramidal geometry at iridium and the hydride in the apical position, the MEP minima were found *trans* to the cyclometallated carbon and having quite close $V_{S,min}$ values [–45.41 (Cl) *vs.* –41.13 (H) for (PCP)IrH(X) and –48.67 (Cl) *vs.* –47.33 kcal mol^{-1} (H) for (PCN)IrH(X)].[34] Opening the H–Ir–H angle lowers the basicity of hydride ligands, *e.g.*, in the resulting T-shaped complexes, $V_{S,min}$ = –39.55 for (PCN)IrH$_2$ and –30.62 for (PCP)IrH$_2$. At the same time, these complexes are characterized by the much higher Lewis acidity of Ir atom [$V_{S,max}$ = 40.91 for (PCN)IrH$_2$ and 36.69 kcal mol^{-1} for (PCP)IrH$_2$ of T-shaped complexes with $V_{S,max}$ = 22.73 and 6.57 kcal mol^{-1} for square pyramidal L-shaped (PCN)IrH$_2$ and (PCP)IrH$_2$ *vs.* 16.25 and 7.61 kcal mol^{-1} for (PCN)IrH(Cl) and (PCP)IrH(Cl) complexes]. These values are in agreement with comparable (or even higher) initial reaction rates of amine–boranes dehydrogenation observed in the presence of hydridochlorides in comparison to dihydrides.[26,36]

Coordination of bases

Thus, the five-coordinated iridium hydridochloride complexes can easily form a new coordination bond with an additional ligand. For example, bubbling CO through a solution of ($^{Bu^t}$PCP)IrH(Cl) **1** gives hexacoordinated **1**·CO complex in a quantitative yield. In this case, only one of the three possible isomers (**1**·CO_a) (Scheme 2), where the carbonyl ligand is in the apical position (*trans* to the hydride ligand), was characterized by single crystal X-ray diffraction analysis but found as disordered.[37] A similar isomer was characterized for complex **4**·MeCN (Table 3).[30]

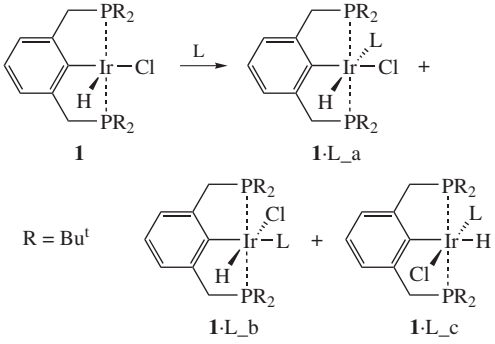

Scheme 2

Table 3 Selected bond distances (Å) and angles (°) for hexacoordinated complexes ($^{Bu^t}$PCP)IrH(Cl)(L) according to single crystal X-ray diffraction data.

Parameter	Complex			
	1·CO	**1**·Py_b	**1**·(4APy)_b	**4**(Ph)·MeCN_a
CCDC no.	745534	1425912	1425913	897997
Reference	37	24	24	30
Ir–H		1.711	1.616	1.579
Ir–Cl	2.475	2.542	2.565	2.475
Ir–C	2.051	2.041	2.031	2.031
Ir–P(1)	2.329	2.331	2.315	2.273
Ir–P(2)	2.329	2.343	2.332	2.273
Ir–L	2.048[a]	2.191[b]	2.190[b]	2.132[c]
H–Ir–Cl	88.8	168.74	172.08	98.61

[a] L = CO. [b] L = N of pyridine. [c] L = N of acetonitrile; **4**(Ph)·MeCN = = (7-6-7-PhPCP)IrH(Cl)(MeCN) complex bearing the PPr$^i_2$ groups.

We have isolated the single crystals of hexacoordinated complexes **1** containing pyridine (Py) and 4-aminopyridine (4APy).[24] In both cases, the pyridine molecule is coordinated equatorially [in *trans* position with respect to the aromatic ring of the pincer (isomer b, see Scheme 2)]. At the same time, NMR studies for a wide temperature range showed that the apical isomer (a) is present in the solution in even higher quantity (the isomer ratio a : b is 2.5 : 1 for both **1**·Py and **1**·4APy).[24,34] In the case of complex **3**, the ratio of isomers is 5 : 1, which can be explained by a lower steric hindrance of the ligand and, consequently, a greater accessibility of the metal center. The *trans* coordination of the hydride and pyridine ligands in the **1**·Py_a–**3**·Py_a complexes was confirmed using pyridine-^{15}N. The signals of apical isomers are broadened at ambient temperatures due to the dissociative exchange, which was slowed down upon cooling. The introduction of ^{15}N label into the ligand causes an additional splitting of the corresponding hydride resonances in ^{1}H NMR spectra: the hydride triplets of **1**·Py_a (δ_{IrH} = –21.64, $^2J_{PH}$ 15.4 Hz) and **2**·Py_a (δ_{IrH} = –21.25, $^2J_{PH}$ 15.7 Hz) are split into pseudo-quartets below 260 K (with $^2J_{NH}$ of 18.2 and 18.6 Hz, respectively), while the signal from **3**·Py_a (δ_{IrH} –23.5) becomes a pseudotriplet at 220 K due to the overlap of two doublets with

$^2J_{N–H} \sim {}^2J_{P–H} \approx 22$ Hz.[24,34] In contrast, the hydride resonances of isomers **1**·Py_b–**3**·Py_b are well resolved even at room temperature. Moreover, the dynamic behavior of the corresponding signals in the ^{31}P NMR spectra repeats that of the hydride resonances.

Another interesting point is that binding of pyridine to complex **2** is non-quantitative at room temperature in contrast to that for **1** and **3**. The residual signals of the starting hydridochloride **2** are observed in the NMR spectra and disappear only at 200 K. The ratio between isomers **2**·Py_a and **2**·Py_b is 24 : 1. This change in the relative stability of complexes with pyridine can be explained by the increase in the Lewis acidity of the iridium atom on going from PCP to POCOP (E_{LUMO} = –1.16 and –1.57 kcal mol^{-1} for **1** and **2**, respectively) and, at the same time, by the decreased availability of the metal center for the coordination of bases.

Variable temperature NMR and UV-VIS spectroscopic studies were performed for both pyridine and aceto- and benzonitriles. The formed hexacoordinated complexes are in equilibrium with starting **1**–**3**, which shifts towards **1**·L–**3**·L in the presence of excess ligand **L** or upon cooling. The nitrile complexes **1**·RCN–**3**·RCN have demonstrated a similar spectroscopic behavior of all hexacoordinated adducts: the dissociative exchange on the NMR time scale for apical isomers leads to the signals broadening at ambient temperatures, allowing their assignment.[34] These studies have also provided thermodynamic parameters (ΔH and ΔS) of formation for each isomer confirming quantitatively the energetic (enthalpic) preference of apical coordination of nitrogen bases. In the case of similar L (PhCN or Py), the stability of isomers changes in the order: (PCP)IrH(Cl)(L) > (EtCOOPOCOP)IrH(Cl)(L) > > (POCOP)IrH(Cl)(L), the ΔH^0 values being from –17 to –5 kcal mol^{-1}.[34] The DFT calculations were in a good agreement with the experimental data and also resulted in higher complexation energies for apical isomers of hexacoordinated complexes (PCP)IrH(Cl)(L) (**1**·L), where L is MeCN, Py, or 2-hydroxymethylpyridine,[25] and (POCOP)IrH(Cl)(L) (**2**·L) or (EtCOO-POCOP)IrH(Cl)(L), where L is MeCN.[34]

According to X-ray diffraction studies, the coordination of the sixth ligand to (PCP)IrH(Cl) complexes **1** and **4** leads to the elongation of Ir–Cl bonds by 0.07–0.14 Å (compare the data in Tables 1 and 3). The DFT calculations performed for a larger set of complexes (**1**·L–**3**·L) confirmed this observation.[25,34] In the case of L = MeCN, the analysis revealed that apical isomers (a) are more stable than the equatorial ones (b) but feature the smaller Ir–Cl bond elongations Δr_{IrCl} (Figure 8). For both isomers, the Δr_{IrCl} values are very similar for the majority of PCP- and POCOP-based complexes, however for the latter, it is achieved at lower complexation energies. That could be correlated with easier activation/higher reactivity of ($^{Bu^t}$POCOP)IrH(Cl).

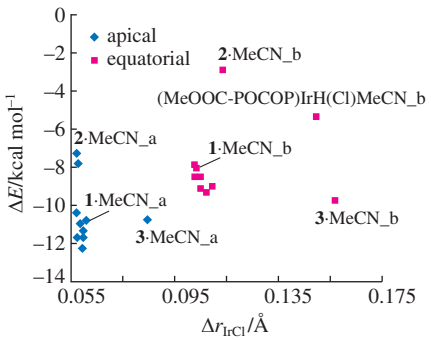

Figure 8 Correlation between the Ir–Cl bond elongation Δr_{IrCl} and complexation energy ΔE for complexes with MeCN. Data for (R–$^{Bu^t}$PCP)IrH(Cl) [where R = 4-H (**1**), OMe, COOMe, F, CF_3, NO_2, or 3,4,5-$(F)_3$], (R–Bu^tPOCOP)IrH(Cl) [R = 4-H (**2**) or COOMe] and (PCN)IrH(Cl) (**3**) from ref. 34.

Table 4 TOFs for dehydrogenation of DMAB and AB catalyzed by Ir^{III} pincer complexes.[a]

Complex	TOF/h^{-1}	
	Me_2NHBH_3[b]	NH_3BH_3[c]
(POCOP)IrH_2	no reaction	1500
(PCN)IrH(Cl)	401	1380[d]
(PCP)IrH(Cl)	80	–

[a] 2 mol% catalyst, room temperature. [b] In toluene. [c] In THF. [d] At 40 °C.

Catalytic dehydrogenation of amine–boranes

As mentioned in Introduction, the (POCOP)-based iridium complexes are very active catalysts of alkane dehydrogenation. Complex ($^{Bu^t}$POCOP)IrH_2 (obtained from **2**) appeared also being an efficient catalyst for the dehydrogenation of ammonia–borane (NH_3BH_3, AB) but has shown no activity in the reaction with dimethylamine–borane ($NHMe_2BH_3$, DMAB).[19] Meantime, hydridochlorides **1** and **3** can catalyze the dehydrogenation of amine–boranes, the activity of ($^{Bu^t}$PCN)IrH(Cl)[29] being higher than that of ($^{Bu^t}$PCP)IrH(Cl)[26] and comparable to that[19] of ($^{Bu^t}$POCOP)IrH_2 (Table 4).

The ^{11}B NMR monitoring of DMAB dehydrogenation in the presence of complexes **1** and **3** revealed different boron containing intermediates: $[Me_2NBHCl]_2$ resulted from the precatalyst activation and Me_2NBH_2 formed *via* dehydrogenation.[26,29] The appearance of latter in the NMR spectra evidences the off-metal formation of the final dehydrogenation product $[Me_2NBH_2]_2$ (Scheme 3).[14,38,39] The important difference between these two catalytic systems is the formation of linear amine–borane dimer intermediate as the result of on-metal dimerization in the case of **3**. That could be the result of lower steric hindrance and higher Lewis acidity of this metal complex leading to the higher stability of metal-bound borohydride intermediates (*vide infra*).

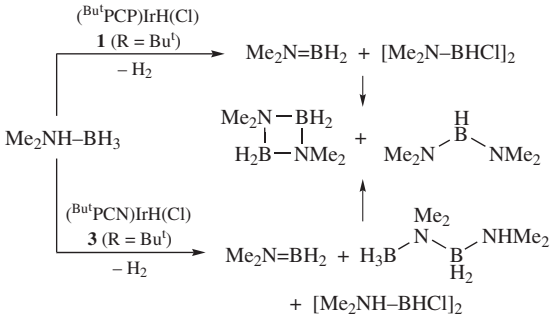

Scheme 3

Variable-temperature (VT) multinuclear NMR and IR investigations of the dehydrogenation reaction mechanism have been performed taking into account the above results on the interaction of iridium pincer complexes with proton donors and bases. Hydrogen bond NH···Cl formation and BH coordination to Ir, which does not occur in the absence of NH functionality,[25] were found among the important first steps of hydridochloride pre-catalyst activation (Scheme 4).[26,29] Interestingly, ^{1}H NMR spectra confirmed the formation of only one isomer of hexacoordinated complex with DMAB in the case of **1**, while complex **3**·DMAB exhibited two hydride signals belonging to apical and equatorial isomers in 8 : 1 ratio, which was also confirmed by DFT calculations.[26,29] The formation of these complexes causes the substantial Ir–Cl bond elongation (by 0.136–0.166 Å). The subsequent Ir–Cl bond dissociation and DMAB dehydrogenation lead exclusively to ($^{Bu^t}$PCN)IrH_4 and cyclic dimer $[BHClNMe_2]_2$.

The apical and equatorial isomers, analogues of **1**·DMAB and **3**·DMAB, have been DFT optimized for the corresponding

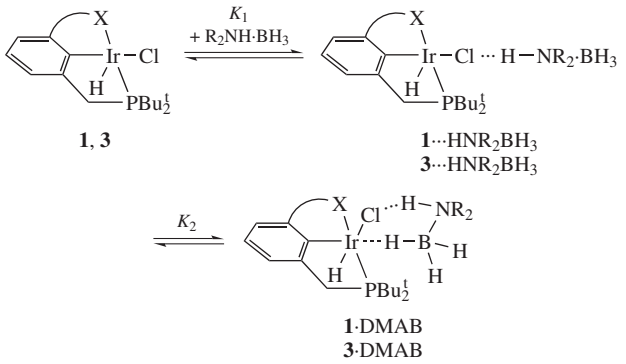

Scheme 4

dihydrides (PCX)IrH_2. Since the dihydrides retain the electronic properties of hydridochlorides, their complexes with DMAB possess the similar structures. For both dihydrides we considered and the model catalysts (MeO–^{Pri}PCP)IrH_2, (^{Me}POCOP)IrH_2, and (^{But}POCOP)IrH_2 reported by other authors,[40,41] the simultaneous η^1-BH coordination and N–H···H–Ir dihydrogen bonding activate the involved bonds and determine the six-membered configuration of the subsequent transition state (Figure 9). Notably, in the case of more sterically demanding [^{But}PCPIr] scaffold, the repulsion between the methyl groups of DMAB and the bulky Bu^t groups of the phosphine moiety allows only the equatorial isomer b of (^{But}PCP)IrH_2(DMAB) to be formed, which is an intermediate in the so-called equatorial catalytic cycle proceeding as concerted proton hydride transfer ($TS_{NH/BH}$, Scheme 5). Formation of apical isomer for less hindered (^{But}PCN)IrH_2 makes the alternative dehydrogenation pathway possible, which proceeds as the stepwise proton (TS_{NH}) and hydride (TS_{BH}) transfers (see Scheme 5). In both cycles, the DMAB dehydrogenation produces tetrahydrido complexes (PCX)IrH_4 and NMe_2=BH_2. However, the sequential proton and hydride transfer in the apical cycle also allow the 'on-metal' amine–borane dimerization[39] to proceed yielding linear diborazane BH_3NMe_2–BH_2NHMe_2 which is observed as a kinetic product of dehydrocoupling (*vide supra*; see Scheme 3). The steric hindrance looks to be the major factor that prevents DMAB binding to the apical site of (^{But}POCOP)IrH_2 as in the case of (^{But}PCP)IrH_2. However, the equatorial DMAB binding is energetically unfavorable.[40] This explains the absence of catalytic activity of this complex in BH_3NHMe_2 dehydrogenation in contrast to the very efficient reaction with unsubstituted BH_3NH_3.[19] Finally, note that the activation energies (ΔG_{TS}) of the equatorial ($TS_{NH/BH}$) and axial (TS_{NH}) cycles for sterically unhindered (^{But}PCN)IrH_2 are very close (13.7 *vs.* 13.1 kcal mol^{-1}), while this energy is much higher (21.0 kcal mol^{-1}) for more hindered (^{But}PCP)IrH_2 causing a lower Lewis acidity of iridium.[29] This difference is in line with their different catalytic activity (see Table 4).

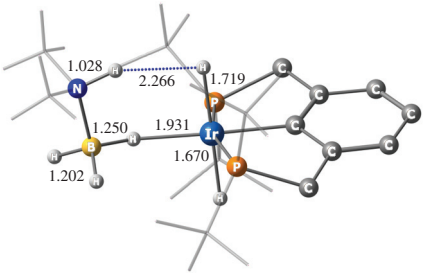

Figure 9 DFT/M06 optimized geometry of hexacoordinated intermediate in the DMAB dehydrogenation catalyzed by complex **1**. Hydrogen atoms of the ^{But}PCP ligand are omitted for clarity, and the Bu^t and Me groups are shown as a wireframe. Figure from ref. 26. ©2017, American Chemical Society. Reproduced with permission.

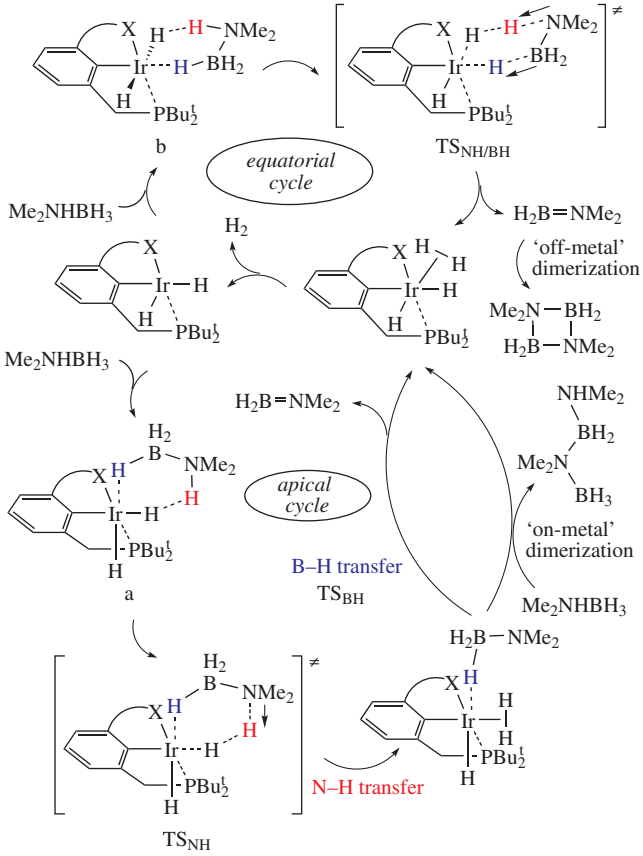

Scheme 5

Conclusions

The benzene-based pincer ligands are the attractive scaffolds, which provide their metal complexes with thermal stability and modularity making them efficient catalysts. Our studies on the square pyramidal iridium hydridochlorides have demonstrated that they are not only convenient precursors to active catalysts, but useful models for the experimental investigations of different processes. As we have summarized herein, the variation of *para*-substituent at the cyclometallated benzene ring affects mostly the electronic properties of the core metal, allowing one to attenuate its Lewis acidity. Change in the *ortho*-substituents from CH_2 to O on going from [(^{But}PCP)Ir] to [(^{But}POCOP)Ir] moieties increases the Lewis acidity, which should consequently lead to a stronger binding of external bases. However, the accompanying change in the complex geometry substantially increases the steric protection of the core metal, which, at the same time, disfavors the formation of hexacoordinated complexes.

These conclusions based on the X-ray structural and computational data were confirmed by the experimental studies. In particular, the dominance of the apical isomers for complexes of pincer iridium hydridochlorides with N-donor ligands has been revealed. Despite the medium strength, which allows one to classify the complexes with pyridine and nitriles as non-covalent, their formation activates the Ir–Cl bonds making the latter ready for dissociation. The energy of N-ligands complexation correlates with the Lewis acidity of iridium atom measured as the maximum of molecular electrostatic potential (MEP maximum, $V_{S,max}$). Thus, the experimentally determined ΔH^0 of complexation can be as well considered as a measure of the metal Lewis acidity.

The non-covalent interactions studied in model reactions with alcohols and bases were determined as the keys to the mechanism of catalytic dehydrocoupling of amine–boranes, which can be performed using pincer iridium hydridochlorides. The reaction is triggered by the formation of NH···Cl hydrogen bond and

subsequent η^1-BH coordination to iridium. These equilibria launch the hydridochloride pre-catalyst transformation into the hydride, which is the real catalyst. In a similar way, the key intermediates in the catalytic cycle are hexacoordinated complexes featuring η^1-BH coordination and N–H···H–Ir dihydrogen bonding. The pincer ligand steric (mostly tuned by substituents at phosphorus) and electronic properties control the feasibility of either equatorial or axial catalytic cycles, wherein the catalytic activity (the reaction barrier) depends on the iridium Lewis acidity as a function of electronic influence of the ligand. These regularities can be generalized for applications to many transition-metal and main-group systems far beyond the amine–boranes dehydrogenation.

This work was supported by the Russian Science Foundation (grant no. 14-13-00801).

References

1 N. V. Belkova, L. M. Epstein, O. A. Filippov and E. S. Shubina, *Chem. Rev*., 2016, **116**, 8545.
2 O. A. Filippov, N. V. Belkova, L. M. Epstein and E. S. Shubina, *J. Organomet. Chem*., 2013, **747**, 30.
3 N. V. Belkova, L. M. Epstein and E. S. Shubina, *Eur. J. Inorg. Chem*., 2010, 3555.
4 N. V. Belkova, O. A. Filippov and E. S. Shubina, *Chem. Eur. J*., 2018, **24**, 1464.
5 P. A. Dub and J. C. Gordon, *ACS Catal*., 2017, **7**, 6635.
6 P. A. Dub, N. J. Henson, R. L. Martin and J. C. Gordon, *J. Am. Chem. Soc*., 2014, **136**, 3505.
7 *Handbook of Hydrogen Energy*, eds. S. A. Sherif, D. Y. Goswami, E. K. Stefanakos and A. Steinfeld, CRC Press, 2014.
8 L. H. Jepsen, M. B. Ley, Y.-S. Lee, Y. W. Cho, M. Dornheim, J. O. Jensen, Y. Filinchuk, J. E. Jørgensen, F. Besenbacher and T. R. Jensen, *Mater. Today*, 2014, **17**, 129.
9 A. Staubitz, A. P. M. Robertson and I. Manners, *Chem. Rev*., 2010, **110**, 4079.
10 W. Lei, D. Portehault, D. Liu, S. Qin and Y. Chen, *Nat. Commun*., 2013, **4**, 1777.
11 Y. Tan and X. Yu, *RSC Adv*., 2013, **3**, 23879.
12 O. T. Summerscales and J. C. Gordon, *Dalton Trans*., 2013, **42**, 10075.
13 H. C. Johnson, T. N. Hooper and A. S. Weller, in *Synthesis and Application of Organoboron Compounds*, eds. E. Fernández and A. Whiting, Springer, Heidelberg, 2015, pp. 153–220.
14 A. Rossin and M. Peruzzini, *Chem. Rev*., 2016, **116**, 8848.
15 O. J. Metters, S. R. Flynn, C. K. Dowds, H. A. Sparkes, I. Manners and D. F. Wass, *ACS Catal*., 2016, **6**, 6601.
16 A. M. Lunsford, J. H. Blank, S. Moncho, S. C. Haas, S. Muhammad, E. N. Brothers, M. Y. Darensbourg and A. A. Bengali, *Inorg. Chem*., 2016, **55**, 964.
17 X. Chen and X. Yang, *Chem. Rec*., 2016, **16**, 2364.
18 M. Gupta, C. Hagen, R. J. Flesher, W. C. Kaska and C. M. Jensen, *Chem. Commun*., 1996, 2083.
19 M. C. Denney, V. Pons, T. J. Hebden, D. M. Heinekey and K. I. Goldberg, *J. Am. Chem. Soc*., 2006, **128**, 12048.
20 M. Albrecht and G. van Koten, *Angew. Chem., Int. Ed*., 2001, **40**, 3750.
21 A. Kumar, T. M. Bhatti and A. S. Goldman, *Chem. Rev*., 2017, **117**, 12357.
22 M. C. Haibach, S. Kundu, M. Brookhart and A. S. Goldman, *Acc. Chem. Res*., 2012, **45**, 947.
23 J. Choi, A. H. R. MacArthur, M. Brookhart and A. S. Goldman, *Chem. Rev*., 2011, **111**, 1761.
24 E. M. Titova, G. A. Silantyev, O. A. Filippov, E. S. Gulyaeva, E. I. Gutsul, F. M. Dolgushin and N. V. Belkova, *Eur. J. Inorg. Chem*., 2016, 56.
25 E. M. Titova, E. S. Osipova, E. S. Gulyaeva, V. N. Torocheshnikov, A. A. Pavlov, G. A. Silantyev, O. A. Filippov, E. S. Shubina and N. V. Belkova, *J. Organomet. Chem*., 2017, **827**, 86.
26 E. M. Titova, E. S. Osipova, A. A. Pavlov, O. A. Filippov, S. V. Safronov, E. S. Shubina and N. V. Belkova, *ACS Catal*., 2017, **7**, 2325.
27 B. Punji, T. J. Emge and A. S. Goldman, *Organometallics*, 2010, **29**, 2702.
28 J. C. Grimm, C. Nachtigal, H.-G. Mack, W. C. Kaska and H. A. Mayer, *Inorg. Chem. Commun*., 2000, **3**, 511.
29 L. Luconi, E. S. Osipova, G. Giambastiani, M. Peruzzini, A. Rossin, N. V. Belkova, O. A. Filippov, E. M. Titova, A. A. Pavlov and E. S. Shubina, *Organometallics*, 2018, **37**, 3142.
30 Y. Shi, T. Suguri, C. Dohi, H. Yamada, S. Kojima and Y. Yamamoto, *Chem. Eur. J*., 2013, **19**, 10672.
31 A. Arunachalampillai, D. Olsson and O. F. Wendt, *Dalton Trans*., 2009, 8626.
32 D. Han, M. Joksch, M. Klahn, A. Spannenberg, H.-J. Drexler, W. Baumann, H. Jiao, R. Knitsch, M. R. Hansen, H. Eckert and T. Beweries, *Dalton Trans*., 2016, **45**, 17697.
33 N. T. Mucha and R. Waterman, *Organometallics*, 2015, **34**, 3865.
34 E. S. Osipova, E. S. Gulyaeva, O. A. Filippov, S. V. Safronov, A. A. Pavlov, A. V. Polukeev, E. M. Titova, E. S. Shubina and N. V. Belkova, *Eur. J. Inorg. Chem*., doi: 10.1002/ejic.201801341.
35 C. Hansch, A. Leo and R. W. Taft, *Chem. Rev*., 1991, **91**, 165.
36 I. Göttker-Schnetmann, P. S. White and M. Brookhart, *Organometallics*, 2004, **23**, 1766.
37 Y. Segawa, M. Yamashita and K. Nozaki, *J. Am. Chem. Soc*., 2009, **131**, 9201.
38 S. Bhunya, T. Malakar, G. Ganguly and A. Paul, *ACS Catal*., 2016, **6**, 7907.
39 A. Kumar, H. C. Johnson, T. N. Hooper, A. S. Weller, A. G. Algarra and S. A. Macgregor, *Chem. Sci*., 2014, **5**, 2546.
40 L. Roy and A. Paul, *Chem. Commun*., 2015, **51**, 10532.
41 A. Paul and C. B. Musgrave, *Angew. Chem., Int. Ed*., 2007, **46**, 8153.

Received: 10th December 2018; Com. 18/5765